CFD Study of Wake Decay and Separation Regions in Jet Engine Test Facilities

Jordan Gilmore and Mark Jermy

Department of Mechanical Engineering,
University of Canterbury, Private Bag 4800, Christchurch, NEW ZEALAND

Abstract

After overhaul or repair, turbofan engines are tested to ensure reliability and thrust meet safe standards. For civil turbofans, these tests are conducted off the wing in indoor test cell facilities. The goal of test cell design is to develop a facility that generates repeatable airflow conditions. Current design and development techniques of jet engine test facilities utilise scaled physical models and 1-D numerical models. With recent development in inexpensive high speed computing recourses, computational fluid dynamics (CFD) has become a attractive method of designing and problem solving within such facilities.

One of the principal issues in modelling test cell flow is the choice of turbulence model. The standard forms of the computationally efficient two-equation models are known to over-predict the length of wakes from bluff bodies in the flow e.g. the beams which support flow conditioning screens. For this application, the Reynolds Stress (RS) linear pressure strain model and LES based models are prohibitive in terms of computational expense.

This work seeks a turbulence model suitable for simulations of test cell flow by tuning the constants of a two-equation RANS model. This is done to gain closer agreement to the downstream wake velocity field produced by a square cylinder disturbance to a uniformly flowing fluid.

The k-ω turbulence model with default parameters is selected as the most appropriate starting point for development. A parametric study suggests that a model with α_∞^* and β_i both set at five times the default value as the best choice for test cell flow studies. This model adequately reproduced the velocity recovery after 4.5 cylinder diameters downstream. It did not reproduce the velocity structure in the recirculation zone immediately downstream of the cylinder. The details of the flow in this recirculation zone have minimal impact on the gross flow in the cell and are of secondary importance in this analysis.

Introduction

The current limitations in computing resources mean that direct numerical solution (DNS) of many industrial flows is not yet attainable at acceptable computational cost. The turbulence properties within smaller length-scales must be estimated as a result. Several computational models belonging to the Reynolds-Averaged Navier Stokes (RANS) family of methods achieve this. The most widely used of these is the semi-empirical k-ε model based on the transport equations for turbulent kinetic energy (k) and dissipation rate (ε). Recently the k-ω model has been adopted in many applications. It is based on transport equations for k and specific dissipation (ω), which is generally thought of as ε/k.

Exacerbated by compromises made to achieve computational efficiency within the RANS models, the accuracy of the solution is often deficient. In order to employ a RANS model to an industrial flow with confidence, extensive validation must be performed. Within the governing RANS model transport equations, a number of modifiable constants exist which affect turbulence dissipation and generation within the solution. The default values of these constants are optimised to perform well in general application to a wide range of flow regimes with reasonable accuracy. The model constants can be tuned to adapt the model to specific flow applications.

The current method of measuring flow consistency in a test cell is through analysis of a velocity distortion (v_{dist}) parameter. This v_{dist} parameter is generated at a analysis plane upstream of the engines inlet face, and is defined by the equation;

$$v_{dist} = \left(\frac{v_{max} - v_{min}}{v_{avg}} \right) \times 100\%$$

Where v_{max}, v_{min}, and v_{avg} are the maximum, minimum and average velocities measured at the analysis plane respectively.

In most test cells, upstream of the analysis plane lies a flow screen which serves to smooth the flow profile, reduce turbulence and prevent damage by foreign objects (FOD). Substantial structural members support these flow screens. These structural members effectively become a bluff body that is detrimental to smooth and consistent cell flow across the cells cross section due to the wake region created in the flow shadow. These wakes impact on downstream elements of the cell. The size and form of these wakes needs to be predicted accurately in order to confidently use CFD as a test cell design and analysis tool.

It is known that both the standard k-ε and k-ω models significantly over predict the stream-wise length of the wake of bluff bodies ([1],[2] and similar observations made in our own work on test cell modelling). Numerous previous studies, including [1], have focussed on employing various wall functions to improve overall accuracy of result in flow around bluff bodies. The work of [1] attempts to eliminate the unrealistically high production of k in areas of stagnation, and applies a two-layer WF to the k-ε model which includes resolution of the near wall viscous sub-layer amongst other work. The present paper investigates what can be done to achieve accurate wake dispersion predictions, for the purpose of test cell modelling, by modifying only the constants of the k-ε and k-ω turbulence models.

Methodology
Computational Package and Test Case

The commercially available CFD code ANSYS Fluent v6.3.26 was used. The test case selected to tune the models was a 2D square cylinder. The 2D square cylinder test case was chosen due to its geometrical similarity to the most common flow screen supports, and in the number of previous studies available in the literature. These include computational studies with RANS, LES, and DES turbulence models, e.g. Xie et al. [3], Lubcke et al. [4], and Rodi et al. [5], as well as experimentally, e.g. Durao et al. [6] and Lyn et al. [7].

The experimental work of [7] was deemed inapplicable as the velocity asymptotes to a velocity lower than the free-stream.
The computational domain was set at comparable dimensions to the similar work of [3], [4] and [5]. The width of the cylinder was set at L=75 mm. The computational domain extended 5L upstream, 15L down-stream, and 7L transversely. The computational domain was broken into sub-domains with use of a

graduated structured mesh of 29500 elements. Gambit 2.2.30 was used for meshing.

The inlet boundary condition (BC) was set as a velocity inlet to achieve Re=21400. This is comparable to the values of 14000 and 21400 used in [6] and [7] respectively. The downstream BC was assigned as a pressure outlet corresponding to 0 Pa gauge. The flow-aligned side BCs were assigned a slip free symmetry condition to avoid any boundary layer influences on the wake.

Steady solutions were not stable so a transient solver was used. As expected, the RANS methods did not in general pick up the vortex shedding behaviour, and the simulation converged to a steady state. To ensure consistency, time-step and duration independence tests were run. Following these tests an 'initialisation' run of 1 sec, over 100 time steps, using a the standard k-ε model was performed. The result of this run was used as the initialisation point for all subsequent test cases, before subsequently solving and time averaging the results with the appropriate turbulence model adaptations. This early work and solution strategy allowed reduced solution times due to the partially solved initialisation points, and gave confidence in the time step independence of the results.

The form of the k and ε transport equations that define the k-ε model are presented below;

$$\frac{\partial}{\partial t}(\rho k) + \frac{\partial}{\partial x_i}(\rho k u_i) = \frac{\partial}{\partial x_j}\left[\left(\mu + \frac{\mu_t}{\sigma_k}\right)\frac{\partial k}{\partial x_j}\right] + G_k + G_b - \rho\varepsilon - Y_M$$

$$\frac{\partial}{\partial t}(\rho\varepsilon) + \frac{\partial}{\partial x_i}(\rho\varepsilon u_i) = \frac{\partial}{\partial x_j}\left[\left(\mu + \frac{\mu_t}{\sigma_\varepsilon}\right)\frac{\partial\varepsilon}{\partial x_j}\right] + C_{1\varepsilon}\frac{\varepsilon}{k}(G_k + C_{3\varepsilon}G_b) - C_{2\varepsilon}\rho\frac{\varepsilon^2}{k}$$

ρ defines material density, u, velocity, μ and μ_t, viscosity and turbulent viscosity respectively, and σ_k and σ_ε, the turbulent Prandtl numbers for k and ε. The G terms represent generation of the k, ε due to mean velocity gradients and buoyancy. C terms are modifiable constants. μ_t expands as following and includes modifiable constant C_μ;

$$\mu_t = \rho C_\mu \frac{k^2}{\varepsilon}$$

All user modifiable constants in the k-ε model are listed below along with their default value;

$C_{1\varepsilon}$=1.44, $C_{2\varepsilon}$=1.92, C_μ=0.09, σ_k=1.0, and σ_ε=1.3

C_μ is directly proportional to the turbulent viscosity, μ_t, which has a direct presence in the transport equations. The constants $C_{1\varepsilon}$ and $C_{2\varepsilon}$ appear solely in the transport equation of ε. $C_{1\varepsilon}$, combined with k and ε, generation terms, and constant $C_{3\varepsilon}$ form what is effectively a 'k dissipation-rate production' (ε production) term;

$$C_{1\varepsilon}\frac{\varepsilon}{k}(G_k + C_{3\varepsilon}G_b)$$

In the 2 dimensional test cases, gravity acts in an out of plane direction, and thus buoyancy effects are neglected, and the above term simplifies to;

$$C_{1\varepsilon}\frac{\varepsilon}{k}G_k$$

The term;

$$C_{2\varepsilon}\rho\frac{\varepsilon^2}{k}$$

is effectively a 'dissipation-rate dissipation' (ε dissipation) term in which modifiable constant $C_{2\varepsilon}$ is present.

The ω transport equation combines with the k transport equation presented below to form the basis of the standard k-ω model.

$$\frac{\partial}{\partial t}(\rho k) + \frac{\partial}{\partial x_i}(\rho k u_i) = \frac{\partial}{\partial x_j}\left[\left(\mu + \frac{\mu_t}{\sigma_k}\right)\frac{\partial k}{\partial x_j}\right] + G_k - Y_k$$

$$\frac{\partial}{\partial t}(\rho\omega) + \frac{\partial}{\partial x_i}(\rho\omega u_i) = \frac{\partial}{\partial x_j}\left[\left(\mu + \frac{\mu_t}{\sigma_\omega}\right)\frac{\partial\omega}{\partial x_j}\right] + G_\omega - Y_\omega$$

σ_ω represents the turbulent Prandtl number for ω, and the Y terms represent the dissipation of k and ω. μ_t expands in a slightly modified form from the k-ε model to the following;

$$\mu_t = \alpha * \frac{\rho k}{\omega},$$

in which α* is a modifiable constant, and itself has the following expansion;

$$\alpha^* = \alpha_\infty * \left(\frac{\alpha_0 * + \mathrm{Re}_t/R_k}{1 + \mathrm{Re}_t/R_k}\right)$$

where;

$$\alpha_0^* = \frac{\beta_i}{3}$$

Within the above sets of equations, the following modifiable constants are available to the user;

α_∞^*, α_∞, β_∞^*, β_i, R_β, ζ^*, M_{t0}, σ_k, and σ_ω

α_∞^* is evident in the expansion of the α* term, and is directly proportional. The coefficient α* damps the turbulent μ_t causing a low Re correction [8]. Alteration to α_∞^* directly alters the damping of μ_t. The default value is at unity.

α_∞ provides a damping effect to the term G_ω, through the relations;

$$G_\omega = \alpha\frac{\omega}{k}G_k, \text{ and } \alpha = \frac{\alpha_\infty}{\alpha^*}\left(\frac{\alpha_0 + \mathrm{Re}_t/R_\omega}{1 + \mathrm{Re}_t/R_\omega}\right)$$

The default value of α_∞ sits below unity at 0.52.

β_∞^* and β_i enter the transport equations by way of contribution to the dissipation of k and ω terms, Y_k and Y_ω respectively. Y_ω takes the following form;

$$Y_\omega = \rho\beta f_\beta \omega^2$$

where;

$$f_\beta = \frac{1 + 70X_\omega}{1 + 80X_\omega}, \quad X_\omega = \left|\frac{\Omega_{ij}\Omega_{jk}S_{ki}}{(\beta_\infty * \omega)^3}\right|,$$

$$\Omega_{ij} = \frac{1}{2}\left(\frac{\delta u_i}{\delta x_j} - \frac{\delta u_j}{\delta x_i}\right), \text{ and}$$

$$\beta = \beta_i\left[1 - \frac{\beta_i *}{\beta_i}\zeta * F(M_t)\right]$$

Whilst Y_k has the form;

$$Y_k = \rho\beta * f_{\beta*}k\omega$$

where;

$$\beta^* = \beta_i *\left[1 + \zeta * F(M_t)\right], \text{ and}$$

$$\beta_i^* = \beta_\infty *\left(\frac{4/15 + (\mathrm{Re}_t/R_\beta)^4}{1 + (\mathrm{Re}_t/R_\beta)^4}\right)$$

β_∞^* and β_i influence the asymptotic value of ω^+ in the laminar sub-layer for the wall boundary condition treatment of ω. The various wall treatment test cases provided no improvements over the standard models.

M_{t0} is related to compressibility corrections. The velocities dealt with in this analysis lie far from the effects of compressibility. Thus, M_{t0} alterations were ignored in this analysis. Sample trials with variations in R_β and ζ^* showed a negligible influence on the results, and are not included in the results section below.

Initial Tests of Standard Fluent Models and Features
Initial tests with the standard Fluent turbulence model variants, wall functions, and discretisation schemes were performed. In addition the effect of inlet turbulence intensity was analysed. From the preliminary work, a solution strategy for the initial tests was developed. This consisted of running each case for an additional 200, 0.01 sec time steps from the above mentioned initialisation point. All but those solutions exhibiting vortex shedding reached a steady state by this point. Due to the presence of vortex shedding in several of the test cases, a consistent

approach of time averaging the results was adopted. For the initial test cases, data was taken at every 5-time steps over the final 2 seconds of solution time, and then time averaged. As inlet turbulence was tested as a variable during these initial tests, the default inlet turbulence levels of 10% turbulence intensity (TI), and 1 m length scale were used in place of the experimental inlet turbulence conditions of [6] that were later adopted for the turbulence model tuning process.

The standard turbulence model variations tested were; The 2 equation k-ε model in the standard, realizable, and RNG forms, and the k-ω in the standard and SST forms. Additionally the Reynolds Stress (RS) linear pressure strain model was analysed for comparative purposes during the initial stages.

The standard k-ε model was tested with the 'non-equilibrium' and 'enhanced' wall functions (WFs). No improvement was seen over the standard model at this Re, and the default WF was used in all subsequent tests. The spatial discretisation schemes, 1st, 2nd and 3rd order MUSCL, along with Power and QUICK variants were also tested. The effects in the sample case were negligible, and as such the more detailed tuning stages of the analysis used the most computationally efficient 1st order scheme.

Second Stage Investigation of Standard Fluent Turbulence Models

In tests of the unmodified standard models, the standard version of the k-ω model provided significantly more accurate results than the SST k-ω model. Little difference in accuracy was seen between the variants of the k-ε model tested (standard, realizable, and RNG). The standard k-ε and k-ω models were selected for the next stage of analysis, which included 'tuning' of the modifiable constants.

The inlet BC for this stage of the investigation was set to match those of [6] with TI=6%. The length scale was modified to 1.05 m. This matched the characteristic length of the effective duct created by the symmetry BCs imposed upon the stream-wise edges of the computational domain. The time-step and run duration were refined from the initial analysis. All models were run for 2 seconds over 200-time steps with the test case turbulence model settings as a settling period. This was performed from the same partially solved initialisation point used in the initial tests. A further 300, 0.01 sec time steps were performed with data sampling performed every fifth time iteration, and the results time averaged.

A parametric study was performed. Each of the modifiable turbulence model constants was altered to 50% and 200% of the default value. The results of the k-ε model were not investigated after this stage. The k-ω models far downstream accuracy improvements were seen to be more encouraging. The model constant modifications with positive influence on the accuracy of the results were identified as decreases in α_∞ and β_∞^*, and increases in α_∞^* and β_i.

Third Stage Investigation of Standard Fluent Turbulence Models

A more detailed analysis of the constant modifications to the turbulence model constants α_∞, β_∞^*, α_∞^*, and β_i was performed. Computational runs were performed with single constant modifications of 20% and 10% of the default value for α_∞ and β_∞^*, and at 500% and 1000% for α_∞^*, and β_i. α_∞ and β_∞^* were not decreased below 0, as doing so would convert k and ω dissipation terms into generation terms and vice versa. Modification of α_∞^* and β_i provided superior results, as the upper bound to which they could be modified was not restricted in this analysis.

Fourth Stage Investigation of Standard Fluent Turbulence Models

A final 'tuning' step was performed to best match the experimental work of [6] for purposes of applying Fluent commercial CFD code to test cell analysis. Through the previous investigation stages, it was observed that the accuracy of the prediction (1) in the recirculation zone immediately downstream of the cylinder, and (2) in the dispersion of the wake further downstream had not been improved simultaneously. The best results of the stage three analysis were combined for a fourth stage of optimisation. Multiple combinations of simultaneous changes in constants α_∞^* and β_i were performed. With the downstream wake at the desired level of accuracy further modifications were performed in an attempt to improve the near wake region in the immediate vicinity of the cylinder. Earlier results indicated that decreases in β_i, and increases in α_∞ and β_∞^* produced significantly higher velocities in the immediate downstream recirculation region behind the cylinder. As a result of these changes, the recirculation in this region was suppressed. Finally, as increases in β_i and β_∞^* had already been used to optimise the solution, the influence of including an additional decrease in α_∞ was analysed.

Results
Standard Fluent Turbulence Models

The results of the standard Fluent turbulent 2 equation and 5 equation models applied in the square cylinder test case are presented below in Figure 1 alongside the experimental work of [6]. The data of [6] was obtain by LDV. The authors of [6] estimate the maximum random errors to be, 3.0 and 0.5% for variance and mean values respectively with systematic errors being negligible.

The stream-wise component of velocity along the centre line is plotted. Velocity is non-dimensionalised with free-stream velocity, and distance is non-dimensionalised with cylinder diameter. As noted earlier the data of [7] was deemed inapplicable as the velocity converges to a value lower than that of the free-stream.
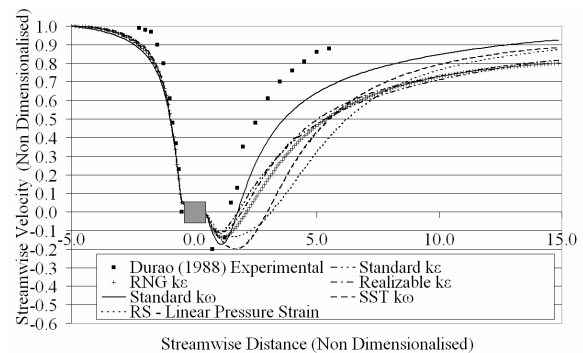

Figure 1 Standard Fluent Turbulence Models

Of the turbulence models tested, the standard k-ω model provided the best results throughout the wake region. The location and magnitude of the recirculation zone immediately downstream of the cylinder are superior to all models. In the region at downstream distances greater than 3 diameters, which is most important for test cell modelling, the performance far surpasses all other tested models.

The k-ω SST model shows relative high levels of accuracy in the magnitude of recirculation velocities, but is far inferior in terms of placing the recirculation regions centre. The recovery towards

mainstream velocity improves over all models other than the standard k-ω.

The three k-ε variants (standard, realizable, and RNG) performed similarly throughout the wake region, and poorly compared to the standard k-ω model. The wake recovery length is severely over predicted. The realizable and RNG variants show small improvements over the standard model in the recirculation region. All three variations recover to near identical levels of accuracy within 15 diameters downstream of the cylinder. The respective velocity plots of the standard k-ε and k-ω models are presented in Figure 2 and Figure 3.

The RS model performed poorly. In the recirculation region, it was the least accurate of all models, and did not surpass the accuracy of the k-ε variants until distances greater than 7.5 diameters downstream. By 15 diameters downstream, the accuracy levels are comparable to those of the k-ω SST model, yet inferior to these of the standard k-ω model.
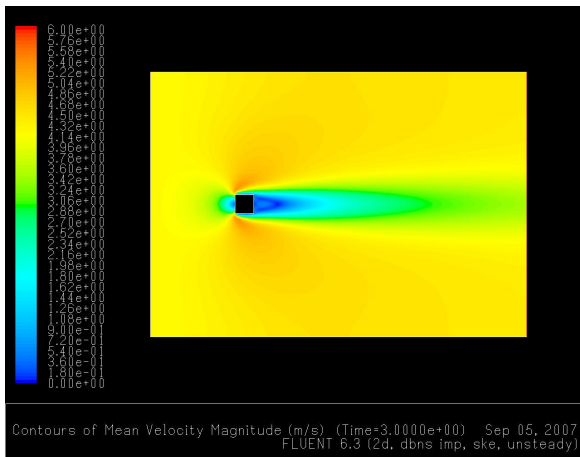
Figure 2 Velocity Contours of Standard k-ε Model Result
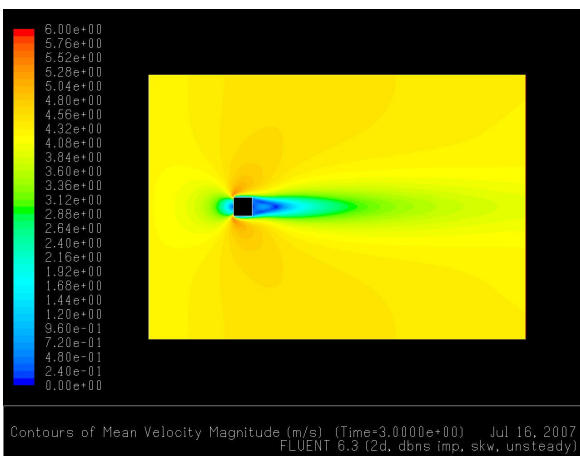
Figure 3 Velocity Contours of Standard k-ω Model Result

Modification to the k-ε Turbulence Model

The results of independent modification to the k-ε model constants is presented in Figure 4 and Figure 5.

Independently decreasing the values of $C_{1\varepsilon}$, and increasing the value of C_μ, $C_{2\varepsilon}$ intensifies all turbulence quantities in both stream wise and transverse directions. Each constant alters the turbulence quantities in a subtly different manner, and the accuracy improvements made reflect this.

Overall the increased mixing which results from increased turbulence produces more rapid wake recovery. Increasing C_μ gave the best accuracy gains by 15 diameters downstream of the cylinder. In the recirculation zone, accuracy is slightly lower than the standard turbulence model. A trend throughout is that accuracy improvements upstream always come at the cost of decreased accuracy in the recirculation zone.
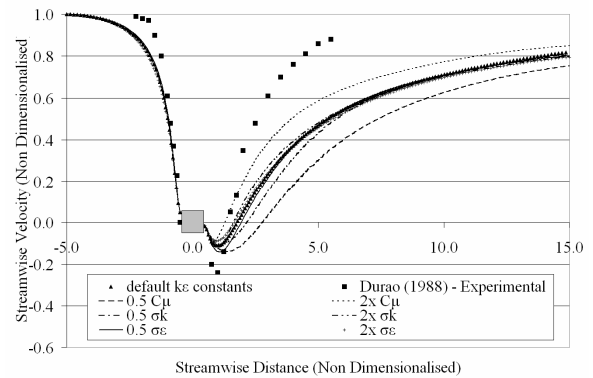

Figure 4 Modifications to the k-ε model – 1

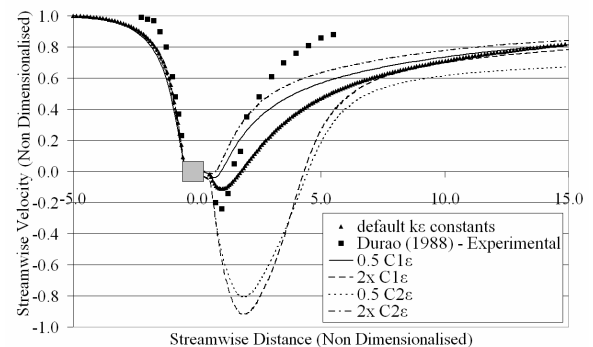Figure 5 Modifications to the k-ε model – 2

Decreases in the value of $C_{2\varepsilon}$, and increases in the value of $C_{1\varepsilon}$, generated vortex shedding. The time-averaged results presented in Figure 5 show a severe increase in the magnitude of the reverse flow within the recirculation zone. This is more severe in the case of $C_{1\varepsilon}$ increase, however, the wake recovery tends towards the accuracy levels of the standard model by 15 diameters downstream.

Increase and decrease of the turbulent Prandtl Number (Pr) in the k and ε equations (σ_k and σ_ε) showed little improvement or degeneration of the solution. By 15 diameters downstream the results are indistinguishable from those produced with the default Fluent settings. Modification to σ_k and σ_ε works in opposition to modifications made to C_μ in the diffusion term of the transport equations. σ_k and σ_ε effectively damp the influence of turbulent viscosity.

No further development of the k-ε model was performed, as k-ω model showed more promise. To further develop the k-ε model to meet the wake recovery requirements of test cell modelling the following recommendations can be made;
Significantly increasing (in the order of 500% of the default value) C_μ in conjunction with a similar size increase to $C_{2\varepsilon}$. These changes will likely increase the wake recovery length to more accurate levels. A trade off of this modification will be the

439

deterioration of accuracy in the recirculation region. To counter this, increasing the value of $C_{1\varepsilon}$ may provide some relief.

Overall the k-ε default Fluent settings provide a good balance between the recirculation and wake recovery regions, as they were designed to do [9]. All RANS turbulence model constant modifications work by increasing or decreasing k and ε generation and dissipation levels. As such, fine-tuning of specific areas of the flow cannot be achieved without impact, often detrimental, upon other areas. However, for the purposes of test cell modelling, the downstream velocities are of primary importance, and the recirculation region secondary.

Modification to the k-ω Turbulence Model
A similar analysis to that presented in the preceding section was performed on the standard k-ω turbulence model. The results are presented in Figure 6 and Figure 7.
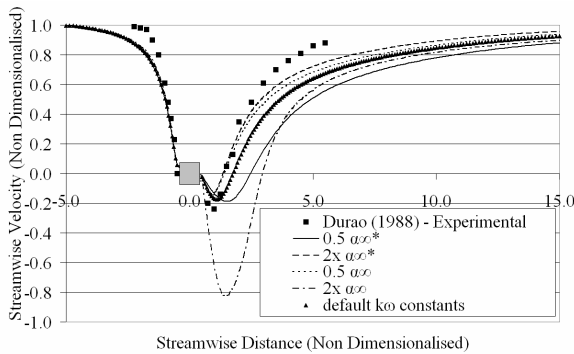
Figure 6 Modifications to the k-ω model – 1
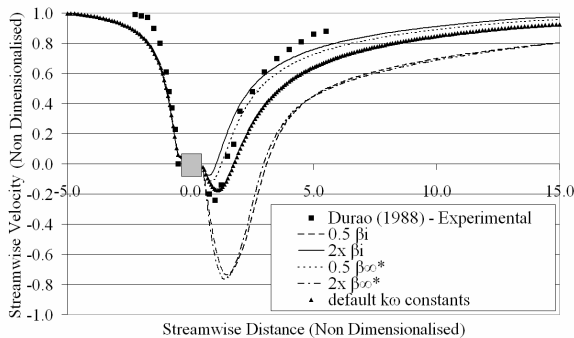

Figure 7 Modifications to the k-ω model – 2

Increased accuracy beyond a downstream distance of greater than 2 diameters was achieved in several instances by independent decreases to constants α_∞, and β_∞^*, and increases to α_∞^*, and β_i. As observed with the k-ε model, these accuracy increases come at the cost of poor accuracy in the recirculation zone. For the purpose of overall wake remixing length accuracy alone, this is an acceptable trade-off. Increases to the constant β_i show the best results at 15 diameters downstream.

No modifications of the k-ω model generated the transient vortex shedding observed with the modified k-ε model. However, the extreme reverse flow velocities, and larger recirculation zone were again observed with decreases to β_i, and increases to α_∞ and β_∞^*. A decrease to α_∞^* moved the centre of the recirculation zone noticeably further downstream than the standard model. Accuracy in recirculation velocity magnitude was improved beyond the levels of all other variations.

Tuning and Wake Dissipation Length Optimisation of the k-ω Turbulence Model
The independent decreases to constants α_∞ and β_∞^*, and increases to α_∞^* and β_i were identified in the preceding analysis step as a good basis for further modification to increase accuracy in overall wake length prediction. The results of more detailed analysis that further explored changes to each individual constant are presented in Figure 8 and Figure 9.

Continual lowering of constants α_∞ and β_∞^* showed that potential improvement reached a plateau prior to the achieving the required accuracy levels. Both constants have a lower limitation on their reduction at 0. Decreasing the value to a level below this alters the transport equations by transforming k and ω generation terms into dissipation terms and vice versa. In the case of α_∞, the generation of ω term, G_ω, would become negative due to the directly proportional relationship between the two quantities. β_∞^* has a directly proportional relationship with Y_k, the dissipation of k. Similarly, transforming this quantity to a negative results in k production and compromises the validity of the transport equations.

Increasing the values of α_∞^* and β_i showed notable increases in accuracy. Raising the level of β_i again showed the most accurate results, and showed potential for further increases. The β_i term finds its way into the transport equation via influence on the ω dissipation term, Y_ω. An increase in β_i increases the value of Y_ω, which effectively becomes the specific generation of k, due to the 'dissipation of ω dissipation' relation.
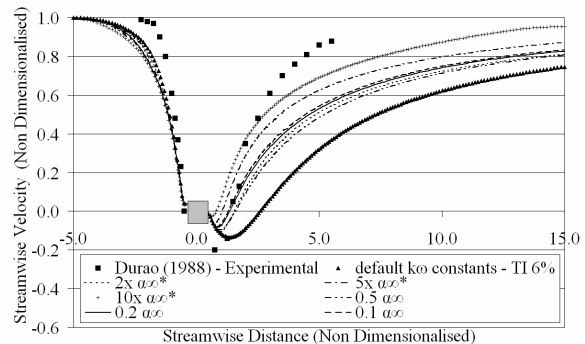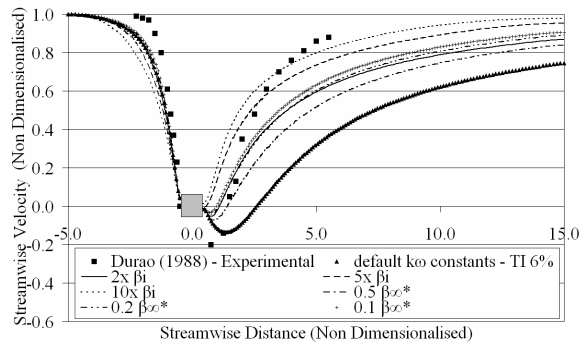

Figure 8 Step 1 of k-ω Constant Optimisation – 1

Figure 9 Step 1 of k-ω Constant Optimisation – 2

The combined far downstream accuracy increases of α_∞^* and β_i modifications were analysed. A number of combinations were tested. The results of the most accurate combinations are presented below in Figure 10. The contour plot of the most accurate downstream result attained is compared to the standard k-ω model result with the inlet turbulence BC of [6] in Figure 11

and Figure 12. The deterioration of the immediate downstream wake recirculation region is demonstrated in the visuals of Figure 13 and Figure 14. Again it is noted that this is of secondary importance in this study.
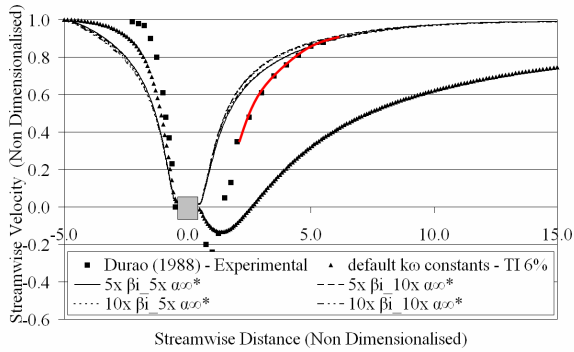

Figure 10 Combined α_∞^* and β_i Constant Modifications

The accuracy of the two constant modification neared a plateau at the level presented in Figure 10. The computational results intersect the experimental results of [6] 4.5 diameters downstream of the cylinder. The computational results continue to follow the experimental data until these data terminate, 5.5 diameters downstream. The most accurate computational solutions are produced from proportionally similar increases in both constants, α_∞^* and β_i. Increasing a single parameter by a factor greater than the other produced a velocity profile of slightly lower accuracy. Only marginal accuracy developments were achieved between a 5 fold increase in both α_∞^* and β_i, and a 10 fold increase of the same parameters. It is desired that the constants remain as close to the original optimised values set in Fluent. This will allow calculations in other flow regimes to maintain accuracy levels similar to that of the default Fluent set up.

Conclusions

Accurate prediction of the wakes of bluff objects is an obstacle to rapid accurate numerical simulation of the flow in turbofan test cells. A study of boundary conditions, wall models and turbulence models has been carried out. A square cylinder at Re=21400 was used as a test case. The choice of turbulent level at the inlet boundary conditions and the wall function had little effect on the accuracy of prediction of the wake.

Of the two-equation RANS models investigated, with default parameters, the standard k-ω model showed most promise. A parametric study of the model parameters was carried out. Increases of up to fivefold in the constants α_∞^* and β_i improved the accuracy of prediction of the mixing rate and downstream persistence of the wake, adequately reproducing the velocity recovery after 4.5 diameters downstream. This improvement came at the expense of accuracy in the recirculation region immediately downstream of the cylinder, which is of secondary importance in test cell flow. This modified k-ω model will be used in future investigations of the flow in turbofan test cells.
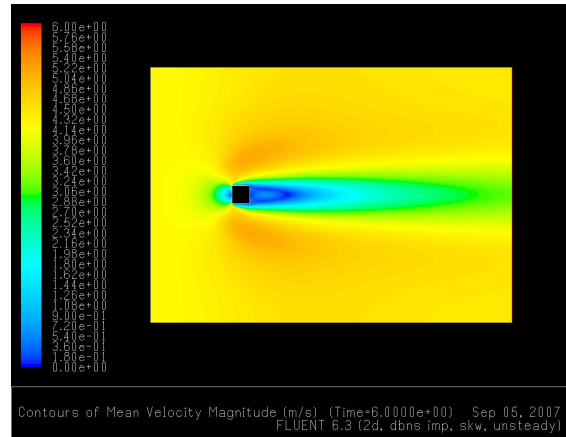

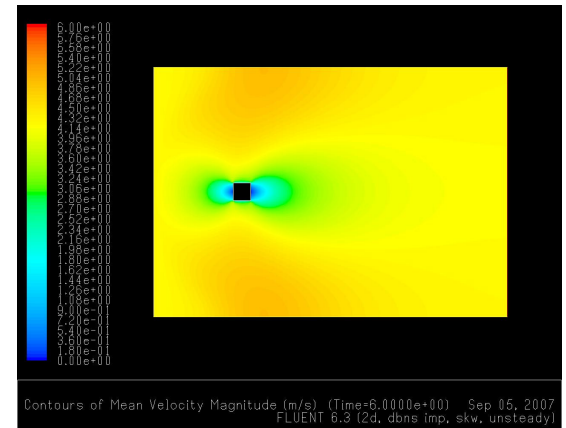Figure 11 Velocity Contours of Standard k-ω Model Result with Inlet Turbulence BC of [6]

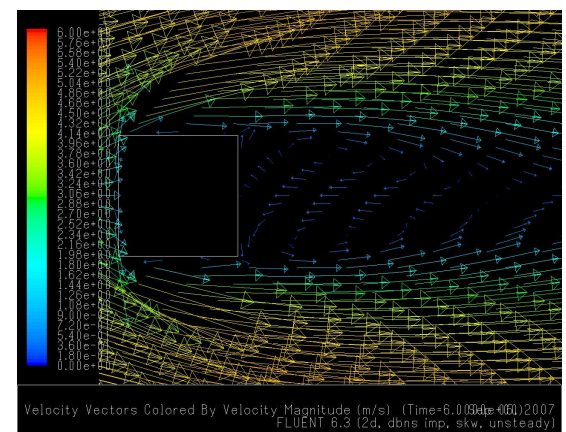Figure 12 Velocity Contours of Optimised k-ω Model Result with 5x α_∞^* and 5x β_i

Figure 13 Velocity Vector Plot of Recirculation Region generated with Standard k-ω Model Result with Inlet Turbulence BC of [6]

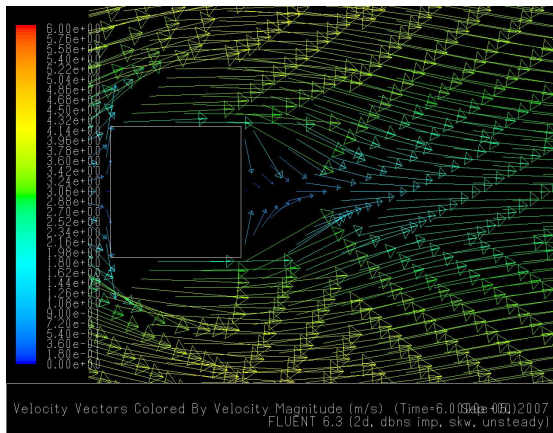Figure 14 Velocity Vector Plot of Immediate Downstream Region of Square Cylinder from Optimised k-ω Model Result with 5x α∞* and 5x βi

References

[1]   W. Rodi, "Comparison of LES and RANS calculations of the flow around bluff bodies," Journal of Wind Engineering and Industrial Aerodynamics, vol. 69-71, pp. 55-75, 1997.

[2]   S. Murakami and A. Mochida, "Turbulent vortex shedding flow past 2D square cylinder predicted by CFD," Journal of Wind Engineering and Industrial Aerodynamics, vol. 54-55, pp. 191-211, 1995.

[3]   Z. Xie, C. Xu, G. Cui, and Z. Wang, "Large eddy simulation of flows around a square cylinder," Jisuan Wuli/Chinese Journal of Computational Physics, vol. 24, pp. 171-180, 2007.

[4]   R. T. Lubcke H. Thiele F, "Comparison of LES and RANS in bluff-body flows," Journal of Wind Engineering and Industrial Aerodynamics, vol. 89, pp. 1471-1485, 2001.

[5]   W. Rodi, J. H. Ferziger, M. Breuer, and M. Pourquie, "Status of large eddy simulation: Results of a workshop," Journal of Fluids Engineering, Transactions of the ASME, vol. 119, pp. 248-262, 1997.

[6]   D. F. G. Durao, M. V. Heitor, and J. C. F. Pereira, "Measurements of turbulent and periodic flows around a square cross-section cylinder," Experiments in Fluids, vol. 6, pp. 298-304, 1988.

[7]   D. A. Lyn, S. Einav, W. Rodi, and J. H. Park, "Laser-Doppler velocimetry study of ensemble-averaged characteristics of the turbulent near wake of a square cylinder," Journal of Fluid Mechanics, vol. 304, pp. 285-319, 1995.

[8]   Fluent, "Fluent v6.3.26 Help Files," 2006.

[9]   B. E. Launder and D. B. Spalding, Lectures in mathematical models of turbulence. London ; New York: Academic Press, 1972.